

Noise Correlations in time- and angular-resolved photoemission spectroscopy

Christopher Stahl and Martin Eckstein

Department of Physics, University of Erlangen-Nuremberg, Staudtstraße 7, 91058 Erlangen, Germany

In time-resolved photoemission experiments, more than one electron can be emitted from the solid by a single ultra-short pulse. We theoretically demonstrate how correlations between the momenta of outgoing electrons relate to time-dependent two-particle correlations in the solid. This can extend the scope of time- and angular-resolved photoemission spectroscopy to probe superconducting and charge density fluctuations in systems without long-range order, and to reveal their dynamics independent of the electronic gap and thus unrestricted by the energy-time uncertainty. The proposal is illustrated for superconductivity in a BCS model. An impulsive perturbation can quench the gap on ultrafast timescales, while non-equilibrium pairing correlations persist much longer, even when electron-electron scattering beyond mean-field theory is taken into account. There is thus a clear distinction between a dephasing of the Cooper pairs and the thermalization into the normal state. While a measurement of the gap would be blind to such pairing correlations, they can be revealed by the angular correlations in photoemission.

ARPES (angular-resolved photoemission spectroscopy) is a powerful technique to probe the electronic structure in solids. With short laser-pulses in a pump-probe setup one can moreover achieve femtosecond time-resolution, which has opened a unique path to explore the light-induced dynamics of collective phases in solids on ultra-short timescales [1]. Time-resolved ARPES has been used to study ultra-fast quasiparticle-dynamics [2, 3], laser manipulation of electronic orders [4–6], photo-induced Mott metal-insulator transitions [7–9], and Floquet Bloch bands [10]. An intriguing aim of the ultra-fast manipulation of condensed matter phases is to control orders like magnetism, charge density waves, or superconductivity. Although the corresponding order parameters are revealed in the electronic spectra, e.g. through the opening of a gap, some fundamental challenges remain to probe their dynamics using ARPES: (i) Spectroscopic probes are limited by the energy-time uncertainty, while the relevant dynamical processes in the destruction or formation of an order parameter ϕ (such as the superconducting condensate density) may be faster than the inverse of the gap Δ which identifies ϕ in the electronic spectrum [38], or happen on the same scale, as for the amplitude mode in superconductors [11–15]. (ii) The quantum state can exhibit strong fluctuations of the order parameter on the nanoscopic scale without forming a long-range order. Such non-equilibrium fluctuations may be an essential property of transient states in which new orders are stimulated by light [16–19], or, as we exemplarily discuss in this work, quenched on a short timescale. A measurement of the spectrum alone would be rather blind to this aspect of the ultrafast dynamics.

Modern time-of-flight detectors for ARPES image outgoing electrons with different momenta onto different pixels of a detector, and thus allow to simultaneously record two electrons which are emitted from a single ultra-short probe pulse into different angular directions. In this paper, we propose that information on time-dependent two-

particle correlations in the solid can be revealed from the correlation between the emission into different directions, i.e., the shot-to-shot noise correlation on the detector. The intriguing potential in measuring noise has been demonstrated in various other settings. For example, noise correlation in time-of-flight measurements of the momentum distribution in ultra-cold gases [20, 21] can distinguish different phases of the initially trapped quantum state, and the shot-to-shot variance of the reflectivity in optical pump-probe experiments has been used to detect squeezing of vibrational modes in a quartz crystal [22], and to measure the current noise in photo-excited Bismuth to probe non-thermal electrons [23].

Two-particle correlations in photoemission have been used previously to study electronic interactions in equilibrium [24–26]. The process discussed here is an emission of two electrons by two photons from the same ultrashort pulse (different from a double photo-emission where one photon leads to the emission of two electrons due to secondary processes), and thus allows a theoretical interpretation along the same lines as the conventional theory for time-resolved photoemission spectroscopy [27–29]. We start from a Hamiltonian $H = H_s + H_e + H'$, where H_s is the Hamiltonian of the solid, and $H_e = \sum_{p\sigma} E_p f_{p\sigma}^\dagger f_{p\sigma}$ describes the emitted electrons with asymptotic momentum p and spin σ ($E_p = p^2/2m + W$, with the work function W). Note that H_s may be time-dependent to incorporate the non-perturbative effect of a probe pulse, or other types of non-equilibrium perturbations. Electron emission is due to the coupling term

$$H' = \sum_{k,p,\sigma,\sigma'} S(t) e^{-i\Omega t} M_{k,p}^{\sigma,\sigma'} c_{k\sigma}^\dagger f_{p\sigma'} + h.c., \quad (1)$$

where $M_{k,p}^{\sigma,\sigma'} \equiv \delta_{\sigma,\sigma'} M_{k,p}$ are matrix elements (for notational simplicity we restrict the solid to one band with electron operators $c_{k\sigma}$), and $S(t)$ is the temporal envelope of the probe with frequency Ω . The Hamiltonian H has built in two basic assumptions which are commonly made in the theory of ARPES: (i) There is no interac-

tion between electrons in outgoing states (f_p) and electrons in the solid (c_k), manifesting the sudden approximation. Furthermore, (ii), we neglect interactions between outgoing electron and space-charge effects, which is controlled by the excitation density. Finally, all illustrating calculations below are based on simple matrix elements $M_{k,p} = M\delta_{k,p}$. This corresponds to full momentum conservation, as in two-dimensional materials where only the momentum parallel to the surface matters. Matrix element effects could easily be reinstated for an interpretation of real experiments.

A time-resolved ARPES measurement records the total population $I_{p\sigma}^{(1)} = \langle n_{p\sigma}^f \rangle_{t=\infty}$ in an outgoing state ($n_{p\sigma}^f = f_{p\sigma}^\dagger f_{p\sigma}$), which is accumulated over the entire probe pulse duration (until $t = \infty$). Because two electrons can be emitted by two photons from the same pulse, we can measure the correlations $\Delta I_{p\sigma,p'\sigma'} = I_{p\sigma,p'\sigma'}^{(2)} - I_{p\sigma}^{(1)} I_{p'\sigma'}^{(1)}$ at $p \neq p'$, with $I_{p\sigma,p'\sigma'}^{(2)} = \langle n_{p\sigma}^f n_{p'\sigma'}^f \rangle_{t=\infty}$. For a weak probe pulse, all signals are obtained using the leading-order time-dependent perturbation theory in the coupling H' , which is 2nd order for $I^{(1)}$ and 4th order for $I^{(2)}$. We assume that at $t = -\infty$ the outgoing states are empty, and the solid is described by its initial density matrix ρ_0^s . Switching to interaction representation in H' yields $I_{p\sigma,p'\sigma'}^{(2)} = \langle \mathcal{S}^\dagger n_{p\sigma}^f n_{p'\sigma'}^f \mathcal{S} \rangle_0$, where $\mathcal{S} = T_t e^{-i \int_{-\infty}^{+\infty} dt H'(t)}$ is the S-matrix, and $\langle \dots \rangle_0$ the initial state expectation value. Because the initial state does not contain outgoing electrons, the leading order expansion of \mathcal{S} and \mathcal{S}^\dagger in terms of H' is second order and must contain both $f_{p\sigma}^\dagger$ and $f_{p'\sigma'}^\dagger$ (both $f_{p\sigma}$ and $f_{p'\sigma'}$) in \mathcal{S} (\mathcal{S}^\dagger), respectively. After the expansion, the expectation value factorizes for the solid and the outgoing states, so that the result can be expressed in terms of one- and two-point Green's functions of the solid, $G(1, 1') = \langle c(1)^\dagger c(1') \rangle_0$ and

$$G(1, 2, 2', 1') = \langle T_t [c(1)^\dagger c(2)^\dagger] T_t [c(2') c(1')] \rangle_0. \quad (2)$$

Here $1 \equiv (k_1, \sigma_1, t_1)$ etc., is short for space-time variables, and T_t ($T_{\bar{t}}$) is the (anti)-time ordering operator for Fermions. Finally all terms can be combined to (see Appendix)

$$I_{p\sigma}^{(1)} = \int d1 d1' M_{1,1'}^{p,\sigma} G(1, 1'), \quad (3)$$

$$I_{p\sigma,p'\sigma'}^{(2)} = \int d1 d1' d2 d2' M_{1,1'}^{p,\sigma} M_{2,2'}^{p',\sigma'} G(1, 2, 2', 1'), \quad (4)$$

where $\int d1 = \sum_{k_1, \sigma_1} \int_{-\infty}^{\infty} dt_1$, and

$$M_{1,1'}^{p,\sigma} = M_{k_1,p}^{\sigma_1,\sigma} (M_{k_1',p}^{\sigma_1',\sigma})^* S(t_1) S(t_1')^* e^{i(E_p - \Omega)(t_1 - t_1')}. \quad (5)$$

The expression for $I_{p\sigma}^{(1)}$ is the conventional expression for time-resolved ARPES [27, 28], which can be understood as a time-dependent filter $M(t, t')$ applied to the single-particle propagator [30]. Equation (4) provides an analogous view on two-particle quantities.

To illustrate the use of noise correlation in time-resolved ARPES, one can consider an ideal ultra-short pulse $S(t) = A\delta(t - t_0)$. In this case, Eqs. (3) and (4) yield $I_{p\sigma}^{(1)} = |AM|^2 \langle n_{p\sigma}^c \rangle_{t=t_0}$ and

$$\Delta I_{p\sigma,p'\sigma'}^{(2)} = |AM|^4 (\langle n_{p\sigma}^c n_{p'\sigma'}^c \rangle - \langle n_{p\sigma}^c \rangle \langle n_{p'\sigma'}^c \rangle)_{t=t_0}, \quad (6)$$

where $n_{p\sigma}^c = c_{p\sigma}^\dagger c_{p\sigma}$ is the momentum occupation, and $\langle \mathcal{O} \rangle_t$ is the expectation value of an operator *in the solid* at time t . The angular correlations thus directly yield the momentum correlations in the solid, which can provide unique information on the state. In the BCS wave function, e.g., $\langle n_{k\uparrow}^c n_{-k\downarrow}^c \rangle - \langle n_{k\uparrow}^c \rangle \langle n_{-k\downarrow}^c \rangle = |\langle c_{k\uparrow} c_{-k\downarrow} \rangle|^2$ is a direct measure of pairing correlations, while $\langle n_{k\sigma}^c \rangle$ remains smooth throughout the superconducting transition.

By looking at different pairs k, k' ($k \neq k'$) in $\Delta I_{k,k'}$, different symmetry broken phases can be characterized (charge-density waves, superconductivity, etc.). In the following we provide an illustrative example for using the noise correlations in the study of superconductivity. We start the discussion from the Hubbard model

$$H = -J \sum_{\langle i,j \rangle, \sigma} c_{i\sigma}^\dagger c_{j\sigma} + U/2 \sum_{i,\sigma} n_{i\sigma} n_{i-\sigma}, \quad (7)$$

which is the paradigmatic Hamiltonian to describe the physics of interacting electrons. Here J is a hopping between nearest neighbor sites on a lattice, and U is an on-site interaction. We choose an attractive interaction $U < 0$, which leads to s-wave superconductivity. To understand the rich non-equilibrium dynamics in superconductors, it is illustrative to recapitulate first the time-dependent mean-field solution. By decoupling the interaction term in the Cooper channel, the BCS-Hamiltonian $H_{BCS} = \sum_k \hat{\psi}_k^\dagger \hat{h}_k \hat{\psi}_k$ is obtained. Here $\hat{\psi}_k = (c_{k\uparrow}, c_{-k\downarrow}^\dagger)^T$ is the Nambu-Spinor and $\hat{h}_k = \hat{\sigma}_z \epsilon_k + \hat{\sigma}_x \Delta' - \hat{\sigma}_y \Delta''$, with the electron dispersion ϵ_k and the gap $\Delta = \Delta' + i\Delta'' = U \sum_k \langle c_{-k\downarrow} c_{k\uparrow} \rangle$. The BCS-Hamiltonian can be written in terms of the Anderson pseudo-spins $\vec{s}_k = \frac{1}{2} \hat{\psi}_k^\dagger \hat{\sigma} \hat{\psi}_k$ [31], which follow the equation of motion $\dot{\vec{s}}_k = \vec{B}_k \times \vec{s}_k$ with the pseudo magnetic field $\vec{B}_k = (2\Delta', -2\Delta'', 2\epsilon_k)$. This defines an integrable set of coupled linear differential equations with an infinite number of conserved quantities [12, 32, 33]. A simple protocol such as a sudden quench or ramp of the interaction can lead to collective amplitude modes or an ultra-fast vanishing of the gap [11, 12]. It must be emphasized that the mean-field-dynamics is highly non-thermal, even after a melting of the gap. For example, after a quench of the interaction to $U = 0$ in H_{BCS} , the gap exponentially decays like $\Delta(t) \sim e^{-2t\Delta(0)}$, while the Cooper-pair correlations $F_k = |\langle c_{-k\downarrow} c_{k\uparrow} \rangle|$ at each k remain nonzero, because the Anderson pseudo-spins \vec{s}_k simply precess at different frequencies, such that the global order only dephases [32]. In contrast, thermalization to a normal state above T_c (e.g., due to electron-electron scattering) would imply $F_k = 0$.

In the following we demonstrate that thermalization and dephasing of superconducting order can be distinct even when realistic electron-electron scattering beyond mean-field theory is taken into account, and that the noise correlations provide a unique measure to distinguish them experimentally. We examine a simple quench or ramp of the interaction, which initiates dynamics representative for a generic impulsive excitation: The final value of U determines the electron-electron scattering and the pairing interaction during the dynamics, while the quench or ramp amplitude mainly sets the excitation density. To incorporate electron-electron scattering beyond mean-field theory, the Hubbard model is solved using non-equilibrium dynamical mean-field theory (DMFT) and an impurity solver based on iterated perturbation theory [34]. We use a semi-elliptic density of states $D(\epsilon)$, where the half-bandwidth $W = 2$ sets the unit of energy and time ($\hbar = 1$). DMFT gives access to all normal and anomalous single-particle Green's function in the lattice, in particular the condensate density $\phi = \sum_k \langle c_{-k\downarrow} c_{k\uparrow} \rangle$ and the individual F_k . Momentum dependent quantities g_k are represented as functions of the band energy $\epsilon_k \in (-2, 2)$ (Fermi energy $\epsilon_F = 0$), and momentum averages are given by the integral $\sum_k g_k \equiv \int d\epsilon D(\epsilon)g(\epsilon)$.

Figure 1a shows the order parameter $\phi(t)$ (solid lines) and the Cooper pair amplitude F_{k_f} (dashed lines) at the Fermi-surface, after a sudden quench of the interaction from an initial value $U_0 = -3$ to $U = U_0 + \Delta U$. For weak excitations ΔU , the order parameter and F_{k_f} oscillate with a small amplitude, while both decays to zero for large ΔU (e.g., dark red lines). In general, F_{k_f} decays much slower than ϕ , even at relatively large interactions and excitations strong enough to melt the gap (see, e.g., the bold curve for $U = -0.6$). Hence there is a large time window where the vanishing of the order parameter ϕ is mainly due to dephasing, in spite of electron-electron scattering. This behavior can be unravelled by the noise correlation measurement. As the condensate of Cooper pairs is formed by electrons with opposite momentum p and $-p$, it is natural to measure the correlations $\Delta I_p \equiv \frac{1}{2} \sum_{\sigma, \sigma'} \Delta I_{p\sigma, -p\sigma'}$. For the BCS-Hamiltonian one could use Wick's theorem to decouple the two-point function (2). The only nonvanishing contribution to the connected Green's function $G(1, 2, 2', 1') - G(1, 1')G(2, 2')$ which enters the fluctuations ΔI_p is therefore related to an anomalous Green's function $\bar{G}_p(t, t') = \langle T_t [c_{p\uparrow}^\dagger(t') c_{-p\downarrow}^\dagger(t)] \rangle$ [c.f. Eqs. (4) and (3)],

$$\Delta I_p = \left| \int dt' dt'' S(t') S(t'') \bar{G}_p(t', t'') e^{i(E_p - \Omega)(t' + t'')} \right|^2, \quad (8)$$

where we set $M_{k,p}^{\sigma_1, \sigma} = \delta_{k\sigma_1, p\sigma}$ as explained above. As long as the system is initially deeply in the symmetry broken phase, these anomalous terms capture the leading

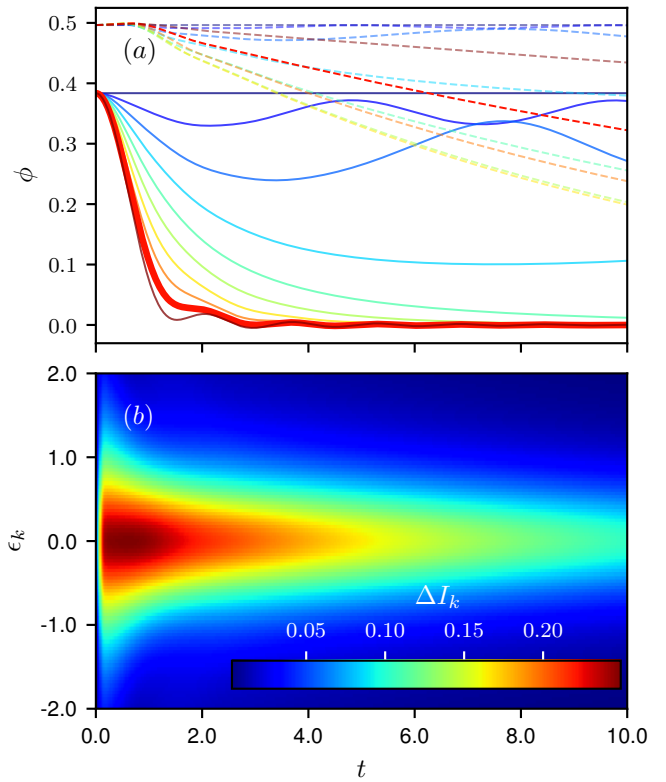


FIG. 1: a) Order parameter ϕ (solid) and pairing correlations F_{k_f} (dashed) at the Fermi surface ($\epsilon_k = 0$) after an interaction quench with $\Delta U = 0.0, 0.3, \dots, 2.7$ (top to bottom). The bold line correspond to $\Delta U = 2.4$. b) Numerical simulation of the noise correlation measurement for $\Delta U = 2.4$: $\Delta I_k(t)$, as obtained from Eq. (8) with a short pulse $S(\tau) = \sqrt{100/\pi} e^{-100(\tau-t)^2}$ centered around time t .

contribution to the two-particle Green's function even beyond mean-field theory (apart from vertex corrections). We therefore simply evaluate Eq. (8) using the DMFT solution. The simulated ARPES noise correlations, shown in the Fig. 1b, directly reveal the presence of Cooper pair correlations beyond the vanishing of ϕ . A complementary tr-ARPES can detect the vanishing of ϕ by the closing of the spectral gap, so that the dephasing of the superconducting state can be identified. Vertex corrections to Eq. (8) would complicate a quantitative prediction of the value of ΔI_k , but the very different timescales for the two and one-particle dynamics should remain a clear signature for experiment.

In the quench protocol, a strong excitation of the system simultaneously implies weak final interactions U . To simulate a strong impulsive excitation at large U , we perform a short pulse-shaped ramp of the interaction of duration τ , $U(t) = U_0 + \Delta U/2\theta(\tau - t)(1 + \cos(\pi t/\tau))$. Figure 2a shows the resulting $\phi(t)$ (solid lines) and F_{k_f} . The relaxation dynamics is analyzed in a regime of relatively large $U = -3$, which is close to the maximum of

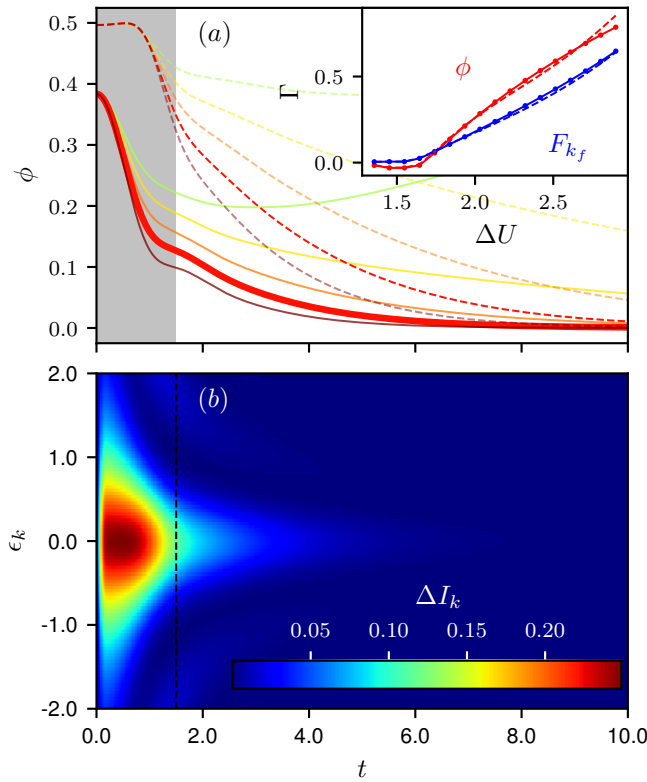


FIG. 2: a) Order parameter ϕ (solid lines) and Cooper pair correlations F_{k_f} (dashed lines) for the ramp protocol with different excitation densities $\Delta U = 1.5, 1.8, \dots, 2.7$ (from top to bottom). The bold line shows $\Delta U = 2.4$. The shaded area highlights ramp duration period. *Inset:* Decay rate Γ obtained by an exponential fit to $\phi(t)$ (solid red), the momentum averaged noise $\sum_k \sqrt{\Delta I_k(t)}$ (dashed red), F_{k_f} (solid blue) and $\sqrt{\Delta I_{k_f}(t)}$ (dashed blue) against ΔU . b) Numerical simulation of the noise correlation measurement $\Delta I_k(t)$ for energies around the Fermi edge for $\Delta U = 2.4$.

the transition temperature $T_c(U)$ in the phase diagram, corresponding to the crossover into the strong-coupling regime of a BEC of preformed pairs. Similar to Fig 1a, amplitude mode oscillations or a melting of the gap are observed depending on the excitation ΔU , but the larger electron-electron scattering now leads to a rapid relaxation of both the order parameter ϕ and F_{k_f} . The decay rates Γ_ϕ and Γ_F of ϕ and of F_{k_f} are of the same order, as shown by the solid lines in the inset of Fig. 2a. (Both Γ_ϕ and Γ_F show a slow-down at the threshold $\Delta U \approx 1.6$ for the melting of the order.) The noise correlations (Fig. 2b), allow to probe the dynamics of these quantities. In particular, by fitting an exponential decay $\exp(-\Gamma t)$ to the simulated data for $\sqrt{\Delta I_k(t)}$ and the momentum average $\sum_k \sqrt{\Delta I_k(t)}$ one can closely recover the corresponding rates Γ_ϕ and Γ_F (inset). In the present case, pairing interactions and scattering are controlled by the same microscopic interaction U , so that the melting happens on timescales still larger than \hbar/Δ , which could be

resolved in tr-ARPES. In general, however, there is no fundamental limitation for how fast ϕ can be quenched to zero, and the noise correlation measurement, which is independent of the spectral information, grants access to the pair correlations on time scales beyond the energy-time uncertainty limitations of tr-ARPES.

In conclusion, we have proposed to use the angular correlations in ARPES to characterize time-dependent two-particle correlations in the solid. The latter can be expected to dominate non-equilibrium states, but are hard to measure with other techniques. Exemplarily, we showed that the dephasing of the individual order parameter fluctuations can dominate the fast decay of superconductivity, even when electron-electron scattering beyond mean-field theory is included. Beyond this example, the noise correlation measurement could be used to probe transient charge-density wave fluctuations (with correlations between momenta that differ by the nesting vector), excitonic correlations, or magnetic order (to provide a different view on intriguing phenomena such as the melting of magnetic order [35]), and possibly help to reveal fundamental phenomena such as a possible non-thermal criticality in solids [36, 37]. In future work, it will also be interesting to monitor transient states which can have enhanced correlations but no long-range. Furthermore, while the example of this paper uses a short probe pulses to reveal more or less instantaneous correlations, the general result Eq. (4) shows that even *dynamical* time and energy-dependent two-particle quantities can be extracted. Another interesting perspective is the measurement of noise correlations during the application of a pulse, e.g., to reveal time-dependent correlations in Floquet driven states. This requires a gauge invariant reformulation of the theory in the presence of an external vector potential, analogous to standard photoemission [29]. In general, we conclude that the measurement of noise correlations in ARPES, though technically challenging, may give unique access to two-particle correlations in solids, which provides information that is indispensable to characterize the spatio-temporal evolution of non-equilibrium states.

We thank U. Bovensiepen and D. Fausti for useful discussions. We acknowledge the financial support from the DFG Project 310335100, and the ERC starting grant No. 716648.

Appendix: Noise correlation Derivation

In this section we derive the general result for noise correlation $\Delta I_{p\sigma,p'\sigma'}$ from fourth order perturbation theory as explained in the main text. We start with the

expression $I_{p\sigma,p'\sigma'}^{(2)} = \left\langle \mathcal{S}^\dagger n_{p\sigma}^f n_{p'\sigma'}^f \mathcal{S} \right\rangle_0$, where

$$\mathcal{S} = T_t e^{-i \int_{-\infty}^{\infty} d\bar{t} H'(\bar{t})} \quad (9)$$

is the S-matrix in interaction representation with respect to H' . Because initial state contain no electrons in the f -states, the only contribution in fourth order will be

$$\begin{aligned} & \frac{1}{4} \left\langle \int_{-\infty}^{\infty} dt_1 \int_{-\infty}^{\infty} dt_2 T_{\bar{t}} [H'(t_1) H'(t_2)] n_{p\sigma}^f n_{p'\sigma'}^f \int_{-\infty}^{\infty} dt_{1'} \int_{-\infty}^{\infty} dt_{2'} T_t [H'(t_{1'}) H'(t_{2'})] \right\rangle_0 \\ &= \sum_{k_1, k_2, k_1', k_2'} \sum_{\sigma_1, \sigma_2, \sigma_1', \sigma_2'} \int_{-\infty}^{\infty} dt_1 \int_{-\infty}^{t_1} dt_2 \int_{-\infty}^{\infty} dt_{1'} \int_{-\infty}^{t_{1'}} dt_{2'} S(t_1)^* S(t_2)^* S(t_{1'}) S(t_{2'}) e^{-i\Omega(t_{1'}+t_{2'}-t_1-t_2)} \\ & \quad \times (M_{k_1, p_1}^{\sigma_1, \tau_1})^* M_{k_2, p_2}^{\sigma_2, \tau_2})^* M_{k_2', p_2'}^{\sigma_2', \tau_2'} M_{k_1', p_1'}^{\sigma_1', \tau_1'} \langle c^\dagger(2) c^\dagger(1) c(1') c(2') \rangle_0^c \otimes \langle f(\bar{2}) f(\bar{1}) f_{p\sigma}^\dagger f_{p'\sigma'}^\dagger f_{p'\sigma'}^\dagger f_{p'\sigma'}^\dagger f_{p'\sigma'}^\dagger f_{p'\sigma'}^\dagger \rangle_0^f, \quad (10) \end{aligned}$$

where we introduced the super-indices $i = (k_i, \sigma_i, t_i)$ and $\bar{i} = (p_i, \tau_i, t_i)$. Due to the restriction of free electrons and the assumption that $|\psi^f\rangle$ is empty, we can evaluate the expectation value over f using Wick's theorem and obtain four terms for $p \neq p'$:

$$\begin{aligned} & \langle f(\bar{2}) f_{p\sigma}^\dagger \rangle \langle f(\bar{1}) f_{p'\sigma'}^\dagger \rangle \langle f_{p\sigma} f_{p'\sigma'}^\dagger \rangle \langle f_{p'\sigma'} c^\dagger(\bar{1}') \rangle + \langle f(\bar{2}) f_{p\sigma}^\dagger \rangle \langle f(\bar{1}) f_{p\sigma}^\dagger \rangle \langle f_{p\sigma} f_{p'\sigma'}^\dagger(\bar{1}') \rangle \langle f_{p'\sigma'} f_{p'\sigma'}^\dagger(\bar{2}') \rangle \\ & - \langle f(\bar{2}) f_{p\sigma}^\dagger \rangle \langle f(\bar{1}) f_{p'\sigma'}^\dagger \rangle \langle f_{p\sigma} f_{p'\sigma'}^\dagger(\bar{1}') \rangle \langle f_{p'\sigma'} f_{p'\sigma'}^\dagger(\bar{2}') \rangle - \langle f(\bar{2}) f_{p\sigma}^\dagger \rangle \langle f(\bar{1}) f_{p\sigma}^\dagger \rangle \langle f_{p\sigma} f_{p'\sigma'}^\dagger(\bar{2}') \rangle \langle f_{p'\sigma'} f_{p'\sigma'}^\dagger(\bar{1}') \rangle. \quad (11) \end{aligned}$$

The expectation value $\langle c^f(\bar{i}) c^{f\dagger}(\bar{j}) \rangle$ is given by $\delta_{\tau_i, \tau_j} \delta_{p_i, p_j} e^{-iE_{p_i}(t_i - t_j)}$. Equation (11) can be reinserted into Eq. (10). After summing over $\tau_1, \tau_{1'}, \tau_2, \tau_{2'}, p_1, p_{1'}, p_2, p_{2'}$ we obtain:

$$\begin{aligned} & \sum_{k_1, k_2, k_1', k_2'} \int_{-\infty}^{\infty} dt_1 \int_{-\infty}^{t_1} dt_2 \int_{-\infty}^{\infty} dt_{1'} \int_{-\infty}^{t_{1'}} dt_{2'} S(t_1)^* S(t_2)^* S(t_{1'}) S(t_{2'}) e^{-i\Omega(t_{1'}+t_{2'}-t_1-t_2)} \\ & \times \left[(M_{k_1, p'}^{\sigma_1, \sigma'})^* (M_{k_2, p}^{\sigma_2, \sigma})^* M_{k_2', p'}^{\sigma_2', \sigma'} \langle c^\dagger(2) c^\dagger(1) c(1') c(2') \rangle_0^c e^{-iE_p(t_2-t_{2'})} e^{-iE_{p'}(t_1-t_{1'})} \right. \\ & + (M_{k_1, p}^{\sigma_1, \sigma})^* (M_{k_2, p'}^{\sigma_2, \sigma'})^* M_{k_2', p'}^{\sigma_2', \sigma'} M_{k_1', p}^{\sigma_1', \sigma} \langle c^\dagger(2) c^\dagger(1) c(1') c(2') \rangle_0^c e^{-iE_p(t_1-t_{1'})} e^{-iE_{p'}(t_2-t_{2'})} \\ & - (M_{k_1, p'}^{\sigma_1, \sigma'})^* (M_{k_2, p}^{\sigma_2, \sigma})^* M_{k_2', p'}^{\sigma_2', \sigma'} M_{k_1', p}^{\sigma_1', \sigma} \langle c^\dagger(2) c^\dagger(1) c(1') c(2') \rangle_0^c e^{-iE_p(t_2-t_{1'})} e^{-iE_{p'}(t_1-t_{2'})} \\ & \left. - (M_{k_1, p}^{\sigma_1, \sigma})^* (M_{k_2, p'}^{\sigma_2, \sigma'})^* M_{k_2', p}^{\sigma_2', \sigma} M_{k_1', p'}^{\sigma_1', \sigma'} \langle c^\dagger(2) c^\dagger(1) c(1') c(2') \rangle_0^c e^{-iE_p(t_1-t_{2'})} e^{-iE_{p'}(t_2-t_{1'})} \right]. \quad (12) \end{aligned}$$

By relabeling the indices in the second ($(1, 1') \leftrightarrow (2, 2')$), third ($(1') \leftrightarrow (2')$), and fourth ($1 \leftrightarrow 2$) term of the integrand, one can rewrite the expression in one integral by reintroducing the time ordering operators and obtain the result given in the main text:

$$\begin{aligned} I_{p\sigma, p'\sigma'}^{(2)} = & \sum_{k_1, k_2, k_1', k_2'} \int_{-\infty}^{\infty} dt_1 \int_{-\infty}^{\infty} dt_2 \int_{-\infty}^{\infty} dt_{1'} \int_{-\infty}^{\infty} dt_{2'} S(t_1)^* S(t_2)^* S(t_{1'}) S(t_{2'}) e^{-i\Omega(t_{1'}+t_{2'}-t_1-t_2)} \\ & \times (M_{k_1, p'}^{\sigma_1, \sigma'})^* (M_{k_2, p}^{\sigma_2, \sigma})^* M_{k_2', p'}^{\sigma_2', \sigma} M_{k_1', p'}^{\sigma_1', \sigma'} \langle T_{\bar{t}} [c^\dagger(2) c^\dagger(1)] T_t [c(1') c(2')] \rangle_0^c e^{-iE_p(t_2-t_{2'})} e^{-iE_{p'}(t_1-t_{1'})}. \quad (13) \end{aligned}$$

For the contribution $I_{p\sigma}^{(1)}$ we follow the same route, but only need to go to a second order expansion as $\langle n_{p\sigma}^f \rangle_0 = 0$ and therefore the only contribution to $I_{p\sigma}^{(1)} I_{p', \sigma'}^{(1)}$ in fourth order comes from the second order expansion:

$$I_{p\sigma}^{(1)} = \sum_{k_1, k_1', p_1, p_1'} \int_{-\infty}^{\infty} dt_1 \int_{-\infty}^{\infty} dt_{1'} S(t_1)^* S(t_{1'}) e^{-i\Omega(t_{1'}-t_1)} (M_{k_1, p_1}^{\sigma_1, \tau_1})^* M_{k_1', p_1'}^{\sigma_1', \tau_1'} \langle c^\dagger(1) c(1') \rangle_0^c \otimes \langle f(1) f_{p, \sigma}^\dagger f_{p, \sigma} f_{p', \sigma'}^\dagger(1') \rangle_0^f, \quad (14)$$

where we use the same index convention as before. Again a expansion of the expectation value over f using Wick's theorem yields a term $\langle f(1)f_{p,\sigma}^\dagger \rangle \langle f_{p,\sigma}f_{p',\sigma'}^\dagger(1') \rangle$, which can be evaluated to $\delta_{p_1,p}\delta_{p_1',p}\delta_{\tau_1,\sigma}\delta_{\tau_1',\sigma'}e^{iE_p(t_1-t_1')}$. After reinserting the Kronecker-deltas and contracting the sums, we arrive at the final expression of the main text:

$$I_{p,\sigma}^{(1)} = \sum_{k_1, k_1', \sigma_1, \sigma_1'} \int_{-\infty}^{\infty} dt_1 \int_{-\infty}^{\infty} dt_1' S(t_1)^* S(t_1') e^{-i\Omega(t_1'-t_1)} (M_{k_1,p}^{\sigma_1,\sigma})^* M_{k_1',p}^{\sigma_1',\sigma'} \langle c^\dagger(1)c(1') \rangle_0^c e^{-iE_p(t_1-t_1')}. \quad (15)$$

As explained in the main text the noise correlation are given by $\Delta I_{p\sigma,p',\sigma'} = I_{p\sigma,p'\sigma'}^{(2)} - I_{p,\sigma}^{(1)} I_{p',\sigma'}^{(1)}$.

[1] C. Giannetti, M. Capone, D. Fausti, M. Fabrizio, F. Parmigiani, and D. Mihailovic, *Advances in Physics* **65**, 58 (2016).
[2] C. L. Smallwood, J. P. Hinton, C. Jozwiak, W. Zhang, J. D. Koralek, H. Eisaki, D.-H. Lee, J. Orenstein, and A. Lanzara, *Science* **336**, 1137 (2012).
[3] J. D. Rameau, S. Freutel, A. F. Kemper, M. A. Sentef, J. K. Freericks, I. Avigo, M. Ligges, L. Rettig, Y. Yoshida, H. Eisaki, J. Schneeloch, R. D. Zhong, Z. J. Xu, G. D. Gu, P. D. Johnson, and U. Bovensiepen, *Nature Communications* **7**, 13761 EP (2016).
[4] F. Schmitt, P. S. Kirchmann, U. Bovensiepen, R. G. Moore, L. Rettig, M. Krenz, J.-H. Chu, N. Ru, L. Perfetti, D. H. Lu, M. Wolf, I. R. Fisher, and Z.-X. Shen, *Science* **321**, 1649 (2008).
[5] T. Rohwer, S. Hellmann, M. Wiesenmayer, C. Sohrt, A. Stange, B. Slomski, A. Carr, Y. Liu, L. M. Avila, M. Kalläne, S. Mathias, L. Kipp, K. Rossnagel, and M. Bauer, *Nature* **471**, 490 EP (2011).
[6] S. Mor, M. Herzog, D. Golež, P. Werner, M. Eckstein, N. Katayama, M. Nohara, H. Takagi, T. Mizokawa, C. Monney, and J. Stähler, *Phys. Rev. Lett.* **119**, 086401 (2017).
[7] L. Perfetti, P. A. Loukakos, M. Lisowski, U. Bovensiepen, H. Berger, S. Biermann, P. S. Cornaglia, A. Georges, and M. Wolf, *Phys. Rev. Lett.* **97**, 067402 (2006).
[8] D. Wegkamp, M. Herzog, L. Xian, M. Gatti, P. Cudazzo, C. L. McGahan, R. E. Marvel, R. F. Haglund, A. Rubio, M. Wolf, and J. Stähler, *Phys. Rev. Lett.* **113**, 216401 (2014).
[9] M. Ligges, I. Avigo, D. Golež, H. U. R. Strand, Y. Beyazit, K. Hanff, F. Diekmann, L. Stojchevska, M. Kalläne, P. Zhou, K. Rossnagel, M. Eckstein, P. Werner, and U. Bovensiepen, *Phys. Rev. Lett.* **120**, 166401 (2018).
[10] Y. H. Wang, H. Steinberg, P. Jarillo-Herrero, and N. Gedik, *Science* **342**, 453 (2013).
[11] H. Krull, D. Manske, G. S. Uhrig, and A. P. Schnyder, *Phys. Rev. B* **90**, 014515 (2014).
[12] R. A. Barankov and L. S. Levitov, *Phys. Rev. Lett.* **96**, 230403 (2006).
[13] A. F. Kemper, M. A. Sentef, B. Moritz, J. K. Freericks, and T. P. Devereaux, *Phys. Rev. B* **92**, 224517 (2015).
[14] F. Peronaci, M. Schiró, and M. Capone, *Phys. Rev. Lett.* **115**, 257001 (2015).
[15] R. Matsunaga, Y. I. Hamada, K. Makise, Y. Uzawa, H. Terai, Z. Wang, and R. Shimano, *Phys. Rev. Lett.*

111, 057002 (2013).
[16] J. Bauer, M. Babadi, and E. Demler, *Physical Review B* **92**, 024305 (2015).
[17] K. Ido, T. Ohgoe, and M. Imada, *Science Advances* **3** (2017).
[18] Y. Lemonik and A. Mitra, *Physical Review B* **96**, 104506 (2017).
[19] N. Dasari and M. Eckstein, arXiv e-prints, arXiv:1808.07450 (2018), arXiv:1808.07450 [cond-mat.str-el].
[20] E. Altman, E. Demler, and M. D. Lukin, *Phys. Rev. A* **70**, 013603 (2004).
[21] I. Bloch, J. Dalibard, and W. Zwerger, *Rev. Mod. Phys.* **80**, 885 (2008).
[22] M. Esposito, K. Titimbo, K. Zimmermann, F. Giusti, F. Randi, D. Boschetto, F. Parmigiani, R. Floreanini, F. Benatti, and D. Fausti, *Nature Communications* **6**, 10249 EP (2015).
[23] F. Randi, M. Esposito, F. Giusti, O. Misochko, F. Parmigiani, D. Fausti, and M. Eckstein, *Phys. Rev. Lett.* **119**, 187403 (2017).
[24] F. O. Schumann, C. Winkler, and J. Kirschner, *physica status solidi (b)* **246**, 1483 (2009).
[25] Y. Pavlyukh, M. Schüler, and J. Berakdar, *Phys. Rev. B* **91**, 155116 (2015).
[26] A. Trützschler, M. Huth, C.-T. Chiang, R. Kamrla, F. O. Schumann, J. Kirschner, and W. Widdra, *Phys. Rev. Lett.* **118**, 136401 (2017).
[27] J. K. Freericks, H. R. Krishnamurthy, and T. Pruschke, *Phys. Rev. Lett.* **102**, 136401 (2009).
[28] M. Eckstein and M. Kollar, *Phys. Rev. B* **78**, 245113 (2008).
[29] A. F. Kemper, M. A. Sentef, B. Moritz, T. P. Devereaux, and J. K. Freericks, *Annalen der Physik* **529**, 1600235 (2017).
[30] F. Randi, D. Fausti, and M. Eckstein, *Phys. Rev. B* **95**, 115132 (2017).
[31] P. W. Anderson, *Phys. Rev.* **112**, 1900 (1958).
[32] E. A. Yuzbashyan and M. Dzero, *Phys. Rev. Lett.* **96**, 230404 (2006).
[33] E. A. Yuzbashyan, O. Tsypliyatayev, and B. L. Altshuler, *Phys. Rev. Lett.* **96**, 097005 (2006).
[34] H. Aoki, N. Tsuji, M. Eckstein, M. Kollar, T. Oka, and P. Werner, *Rev. Mod. Phys.* **86**, 779 (2014).
[35] S. Eich, M. Plötzing, M. Rollinger, S. Emmerich, R. Adam, C. Chen, H. C. Kapteyn, M. M. Murnane, L. Plucinski, D. Steil, B. Stadtmüller, M. Cinchetti, M. Aeschlimann, C. M. Schneider, and S. Mathias, *Science Advances* **3** (2017), 10.1126/sciadv.1602094.
[36] J. Berges, A. Rothkopf, and J. Schmidt, *Phys. Rev. Lett.* **101**, 041603 (2008).
[37] N. Tsuji, M. Eckstein, and P. Werner, *Phys. Rev. Lett.* **110**, 136404 (2013).

- [38] In this case, a subtle deconvolution of the spectrum from the probe envelope in time and frequency, or a suitable pulse shaping of the probe pulse may be needed to extract the relevant dynamical information [30].